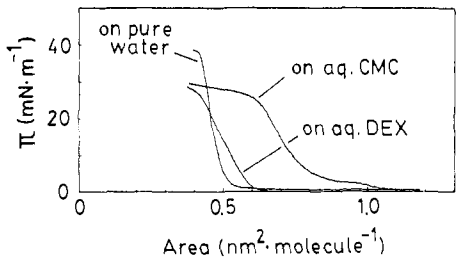

Figure 1. π-A curves of **1** at 20 °C. Polyanion, 1.0×10^{-4} unit M.

Chart I

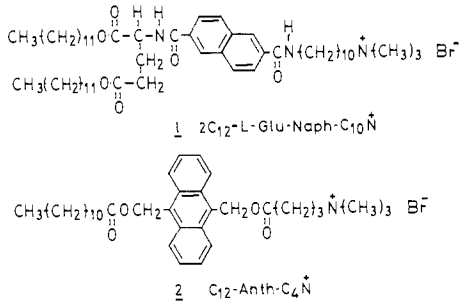

A polyion-complexed monolayer with DEX gives the analogous fluorescence behavior, though with enhanced intensity (1.5–2 times). In contrast, a new emission peak is found on aqueous CMC at 365 nm with vibrational structures at longer wavelengths. This is located in between the monomer-like peak (λ_{max} 354 nm) and the broad excimer peak (λ_{max} 414 nm) of the corresponding aqueous bilayer.[8] Somewhat similar emissions were found for poly(vinylnaphthalenes) and attributed to dimers[14] and second excimers.[15,16] Thus, aqueous CMC produces an expanded monolayer with different naphthalene packing which gives rise to an altered fluorescence pattern.[17]

Energy transfer in monolayers should be controlled by alteration of the chromophore packing. Figure 2b shows fluorescence spectra of naphthalene monolayer **1** containing 1 mol % of anthracene component **2**.[18] On aqueous dextran sulfate, emissions typical of the naphthalene monolayer are observed together with emissions due to the anthracene component at 402 and 424 nm even at low compression. The single-component anthracene monolayer on aqueous polyanions gives broad excimer emissions at 480–490 nm. Therefore, we conclude that the anthracene component in the mixed monolayer exists in the monomeric dispersion and that energy migration among naphthalenes and the subsequent energy transfer to anthracene occur, as illustrated by the insert of Figure 2b. The emission pattern remains the same upon further compression, although the intensity is enhanced.

When the subphase contains CMC, the anthracene emission is not clearly detected. Apparently, the excitation energy is trapped by emission sites of naphthalene (dimers or second excimers) during energy migration and is not efficiently transfered to the anthracene unit.

(14) Irie, M.; Kamijo, T.; Aikawa, M.; Takemura, T.; Hayashi, K.; Baba, H. *J. Phys. Chem.* **1977**, *81*, 1571–1574.
(15) Itagaki, H.; Obukata, N.; Okamoto, A.; Horie, K.; Mita, I. *Chem. Phys. Lett.* **1981**, *78*, 143–146.
(16) Nakahira, T.; Ishizuka, S.; Iwabuchi, S.; Kojima, K. *Macromolecules* **1982**, *15*, 1217–1218.
(17) Blue shifts were observed for the naphthalene ^1B_b band of the surface monolayer relative to that in ethanol, and large hyperchromic effects were found at 300 and 350 nm for the monolayer on pure water and on aqueous DEX but not on aqueous CMC. Fluorescence microscopy studies of the monolayers of **1** containing 0.5% of octadecyl rhodamine B at low surface pressures indicated the presence of crystalline domains on pure water, of noncrystalline islands on aqueous DEX, and of uniform monolayers on aqueous CMC.
(18) The anthracene derivative **2** did not form a stable monolayer on pure water, and a mixed monolayer of **1** and **2** did not display sensitized fluorescence under the same conditions. Thus, all the energy-transfer experiments were conducted on aqueous polyanions. Addition of the anthracene component did not affect the π-A characteristics of **1**.

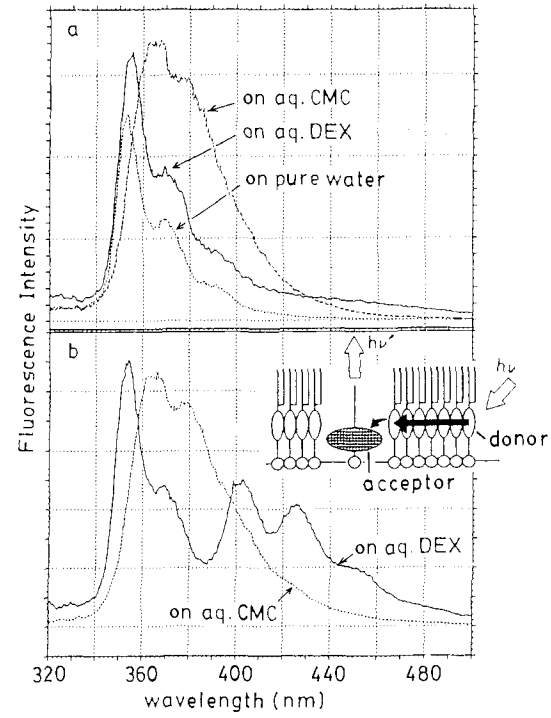

Figure 2. Fluorescence spectra of surface monolayers. Polyanion, 1.0×10^{-4} unit M; 20 °C. a, **1** at 1.0 nm²·molecule⁻¹. The spectral shapes do not change at higher pressures. b, **1**/**2** = 100/1 (mol/mol) at 20 mN·m⁻¹.

In conclusion, we demonstrated directly on water that the altered orientation of the naphthalene monolayer by polyion complexation lead to controlled energy transfer to the anthracene component. Although energy transfer among chromophores in matrix monolayers has been reported,[5,6] the use of self-assembling monolayers with controllable orientation is advantageous as a step toward construction of highly organized, photofunctional molecular systems.

On the Metal Ion Specificity of "Zinc Finger" Proteins

Jeremy M. Berg* and Denise L. Merkle

Department of Chemistry
The Johns Hopkins University
Baltimore, Maryland 21218

Received October 17, 1988

A class of proteins characterized by the presence of one or more sequences of the form Cys-$X_{2,4}$-Cys-X_3-Phe-X_5-Leu-X_2-His-$X_{3,4}$-His (often called "zinc finger" proteins) has been discovered and characterized in recent years.[1-3] Each of these sequences appears to bind a zinc ion in a tetrahedral site formed by the invariant cysteine and histidine residues. The geometry of the site is supported by EXAFS studies[4] and by spectrophotometric studies of Co^{2+}-substituted "zinc finger" peptides[5,6] and of appropriate synthetic model complexes.[7,8] Studies of several of these

(1) Klug, A.; Rhodes, D. *Trends Biochem. Sci.* **1987**, *12*, 464.
(2) Evans, R. M.; Hollenberg, S. M. *Cell* **1988**, *52*, 1.
(3) Berg, J. M. *Met. Ions. Biol. Sys.* **1989**, *25*, 235.
(4) Diakun, G. P.; Fairall, L.; Klug, A. *Nature* **1986**, *324*, 698.
(5) Frankel, A. D.; Berg, J. M.; Pabo, C. O. *Proc. Natl. Acad. Sci. U.S.A.* **1987**, *84*, 4841.
(6) Párraga, G.; Horvath, S. J.; Eisen, A.; Taylor, W. E.; Hood, L.; Young, E. T.; Klevit, R. E. *Science* **1988**, *241*, 1489.
(7) Corwin, D. T., Jr.; Fikar, R.; Koch, S. A. *Inorg. Chem.* **1987**, *26*, 2079.
(8) Corwin, D. T., Jr.; Gruff, E. S.; Koch, S. A. *J. Chem. Soc., Chem. Commun.* **1987**, 966.

0002-7863/89/1511-3759$01.50/0

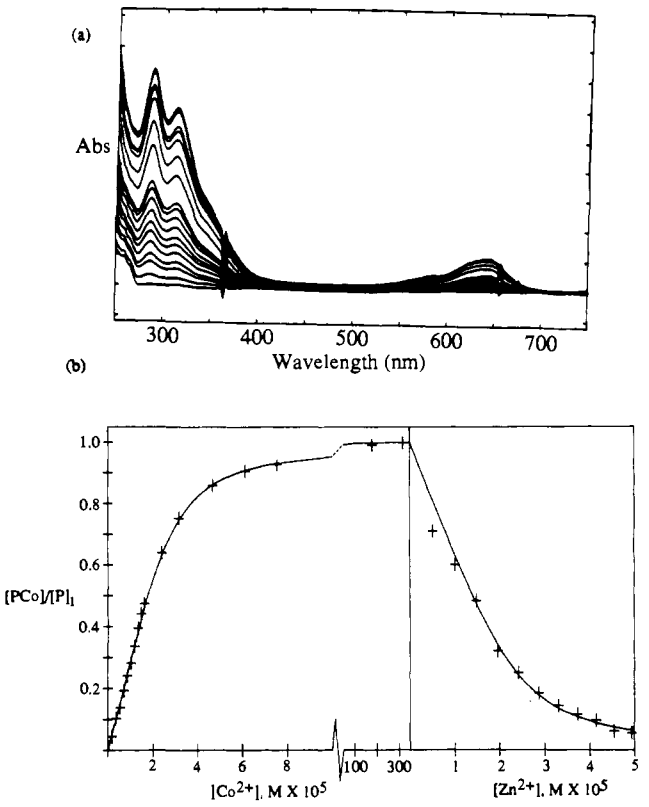

Figure 1. The binding of Co^{2+} to a "zinc finger" peptide. (a) A solution containing 16.2 nmol of the reduced peptide in an initial volume of 500 μL of buffer (20 mM HEPES, 50 mM NaCl, pH 7.00) was titrated with solutions of $CoCl_2 \cdot 6H_2O$ in the same buffer. The reaction was monitored on an HP 8451 diode array spectrophotometer with use of a 1-cm pathlength cell. The titration was performed with degassed solutions under purified dinitrogen. The spectra have been corrected for dilution effects. (b) A plot of the level of saturation of the peptide with Co^{2+} as a function of added Co^{2+} and Zn^{2+} concentrations. The concentration of the peptide–Co^{2+} concentration was determined by using the multicomponent analysis software supplied with the spectrophotometer. The first part of the plot shows the incorporation of Co^{2+} into the peptide derived from the spectra in part (a). The second part shows the effect of added Zn^{2+} on the concentration of the peptide–Co^{2+} complex in the presence of 135-fold excess of Co^{2+}. The curves were fit to the data by using nonlinear least-squares methods.

proteins have revealed that they have specific nucleic acid binding activities that are dependent on the presence of zinc.[9-12] Removal of zinc with chelating agents caused a loss in specific DNA binding activity; addition of Zn^{2+} but not similar concentrations of other metal ions (such as Mn^{2+}, Fe^{2+}, Co^{2+}, Ni^{2+}, and Cu^{2+}) restored activity. We report quantitative metal binding studies of a single "zinc finger" peptide that reveal that this specificity is mirrored by metal binding constants and propose a simple model based on changes in ligand field stabilization energy that appears to provide a rational basis for the specificity for zinc.

Previous studies demonstrated that a "zinc finger" peptide ProPhe**Pro**Cys**Cys**LysGluGluGly**Cys**GluLysGlyPheThrSerLeuHisHisLeuThrArg**His**SerLeuThr**His**ThrGlyGluLys (shown with the metal-binding residues in bold and the invariant hydrophobic residues underlined) undergoes metal ion binding induced folding. This peptide was prepared as described previously.[5] Co^{2+} was selected for initial quantitative binding studies since the spectroscopic properties of its complex with this peptide have been previously examined[5] and since it is the ion most often used in zinc replacement studies.[13] The affinity of the peptide for Co^{2+} was determined by spectrophotometrically monitoring titrations of solutions of the peptide with $Co(OH_2)_6^{2+}$ as shown in Figure 1. With initial peptide concentrations ranging from 5 to 33 μM, the data could be fit using a dissociation constant of $K_d^{Co} = 3.8(\pm 0.5) \times 10^{-6}$ M at pH 7.00 as shown in Figure 1b. Previous studies had indicated that Zn^{2+} will displace Co^{2+} from this peptide.[5] The affinity of the peptide for Zn^{2+} was determined based on the ability of this ion to displace Co^{2+} from the peptide as shown in reaction 1. Titration of the peptide–Co^{2+} complex

$$\text{peptide–}Co^{2+} + Zn(OH_2)_6^{2+} \rightleftharpoons \text{peptide–}Zn^{2+} + Co(OH_2)_6^{2+} \quad (1)$$

with $Zn(OH_2)_6^{2+}$ in the presence of an excess of $Co(OH_2)_6^{2+}$ results in the loss of the absorption spectrum due to the peptide–Co^{2+} complex. An example using 135 equiv of Co^{2+} per peptide is shown in Figure 1b. The data could be fit with a dissociation constant of $K_d^{Zn} = 2.8(\pm 0.9) \times 10^{-9}$ M for the peptide–Zn^{2+} complex using a model in which Co^{2+} and Zn^{2+} compete for the free peptide. The use of the competition procedure provides a convenient spectroscopic basis for monitoring the binding of zinc to the peptide and also provides sufficient curvature in the titration plot so that the dissociation constant for zinc may be determined.

The binding of a metal ion to a peptide of this sort is accompanied by a transition from an octahedral environment in the hexaquo complex to a tetrahedral environment in the peptide binding site. Such a process will involve changes in the ligand field stabilization energy (LFSE), the energy associated with differential destabilization and occupation of d orbitals in a complex with a particular geometry.[14] For the d^7 Co^{2+} ion in a high spin octahedral complex the LFSE is approximately $-4/5$ Δ_o, whereas for a tetrahedral complex it is $-6/5$ Δ_t where Δ_o and Δ_t are the splittings between the sets of d orbitals in octahedral and tetrahedral ligand fields, respectively. For the corresponding Zn^{2+} complexes the LFSE values are zero since this ion has a completely filled d shell. Using values for Δ_o of 9300 cm^{-1} for $Co(OH_2)_6^{2+}$[15] and Δ_t of 4900 cm^{-1} for Co^{2+} in a tetrahedral N_2S_2 environment,[16] the change in LFSE accompanying the exchange reaction 1 is $-21.3 - (-16.8)$ kcal/mol = -4.5 kcal/mol. This is quite similar to the experimentally determined free energy difference for reaction 1 of $\Delta G^{ex} = -RT \ln (K_d^{Co}/K_d^{Zn}) = -4.3$ kcal/mol. The entropy change accompanying reaction 1 is expected to be quite small since it is a simple exchange reaction. This assumption is supported by studies of the thermodynamic properties of a series of MBr_4^{2-} complexes.[17] Thus, the loss of LFSE concomitant with the change from an octahedral to a tetrahedral coordination geometry appears to be a dominant factor that disfavors binding of Co^{2+} over Zn^{2+}. Similar arguments indicate that LFSE effects will similarly disfavor binding of other divalent metal ions Fe^{2+}–Cu^{2+} to such a tetrahedral site. The importance of the LFSE term is further supported by preliminary studies that indicate that Mn^{2+} which has a half-filled d shell and hence no LFSE in high-spin complexes also binds to the peptide more tightly than Co^{2+} does. Furthermore, inspection of lane E2 in Figure 4 from ref 9 reveals that addition of Mn^{2+} to EDTA-treated transcription factor IIIA partially restored specific binding to a 5S RNA gene, whereas addition of Co^{2+}, Fe^{2+}, and Ni^{2+} to the same concentration did not.

Differences in ligand field stabilization energy between octahedral and tetrahedral sites have previously been shown to be important in several contexts. For example, differences in LFSE

(9) Hanas, J. S.; Haruda, D. J.; Bogenhagen, D. F.; Wu, F. Y.-H.; Wu, C.-W. *J. Biol. Chem.* **1983**, *258*, 14120 (1983).
(10) Kadonaga, J. T.; Carner, K. R.; Masiarz, F. R.; Tjian, R. T. *Cell* **1987**, *51*, 1079.
(11) Nagai, K.; Nakaseko, Y.; Nasmyth, K.; Rhodes, D. *Nature* **1988**, *332*, 284.
(12) Eisen, A.; Taylor, W. E.; Blumberg, H.; Young, E. T. *Mol. Cell. Biol.* **1988**, *8*, 4552.
(13) Bertini, I.; Luchinat, C. *Adv. Inorg. Biochem.* **1984**, *6*, 71.
(14) Orgel, L. *An Introduction to Transition-Metal Chemistry*; John Wiley and Sons: New York, 1960.
(15) Figgis, B. *Introduction to Ligand Fields*; Interscience: New York, 1966.
(16) This value was estimated from the spectrum of bis(2,4,6-triisopropylbenzenethiolate)bis(*N*-methylimidazole)cobalt(II)[8] and is entirely consistent with the spectrum of the peptide–Co complex.
(17) Biachi, A.; Paoletti, P. *Inorg. Chim. Acta* **1985**, *96*, L37.

have been found to correlate with the distribution of ions in tetrahedral and octahedral sites in crystal lattices[15] and with the variations in heat released upon dissolving a series of MCl_4^{2-} salts ($M = Mn^{2+}$–Zn^{2+}) in water,[18] a process involving a tetrahedral to octahedral transition. Studies of the copper protein azurin[19] have revealed that apparent metal affinities did not correlate well with changes in LFSE assuming an octahedral to tetrahedral conversion, a fact ascribed to the highly distorted nature of this metal-binding site. Our results suggest that the LFSE changes incumbent in binding metal ions in tetrahedral sites in proteins is an important determinant in specificity for zinc over other divalent first-row transition metals. This observation pertains to the "zinc finger" proteins and to other proteins that appear to have metal ions bound in tetrahedral sites formed from short stretches of amino acid sequence such as the bacteriophage gene 32 protein[20] and the steroid receptor family[21] as well as to other proteins with tetrahedral sites.

Acknowledgment. The National Institutes of Health (BRSG SO7 RR7041, GM-38230) and the Camille and Henry Dreyfus Foundation are gratefully acknowledged for their support of this work.

(18) Blake, A. B.; Cotton, F. A. *Inorg. Chem.* **1964**, *3*, 5.
(19) Engeseth, H. R.; McMillin, D. R. *Biochemistry* **1986**, *25*, 2448.
(20) Giedroc, D. P.; Keating, K. M.; Williams, K. R.; Konigsberg, W.; Coleman, J. E. *Proc. Natl. Acad. Sci. U.S.A.* **1986**, *83*, 8452.
(21) Freedman, L. P.; Luisi, B. F.; Korszan, Z. R.; Basarappa, R.; Sigler, P. B.; Yamamoto, K. R. *Nature* **1988**, *334*, 543.

Nickel-Catalyzed Cyclodimerization of [5]Cumulene (Hexapentaene). Synthesis of a Novel [4]Radialene System

Masahiko Iyoda,* Yoshiyuki Kuwatani, and Masaji Oda

Department of Chemistry, Faculty of Science
Osaka University, Toyonaka, Osaka 560, Japan

Received December 20, 1988

Although the cyclooligomerization of allenes using nickel catalysts has been investigated in detail,[1,2] only a few examples are known of the nickel-catalyzed cyclooligomerization of higher cumulenes. Recently, we have reported the nickel-catalyzed cyclodimerization and trimerization of [3]cumulenes (butatrienes).[3] The cyclooligomerization of [3]cumulenes has importance in organic synthesis, because this reaction provides access to novel compounds of potential theoretical and synthetic interest. We now report a nickel-catalyzed cyclodimerization of [5]cumulenes (hexapentaenes), which produce unique [4]radialene derivatives.

Tetra-*tert*-butyl[5]cumulene (3,8-di-*tert*-butyl-2,2,9,9-tetramethyldeca-3,4,5,6,7-pentaene) dimerizes thermally at 200 °C to give tetrakis(di-*tert*-butylvinylidene)cyclobutane as the cyclic dimer. In contrast, copper-catalyzed decomposition of the anion derived from tetrahydropyranyl ether of 3-hydroxy-3-methyl-1-butyne produces octamethylcyclododeca-1,3,7,9-tetrayne via [6 + 6]cyclodimerization of the corresponding [5]cumulene, which is formed through the coupling of isobutenylidenecarbene.[5] The formation of the cyclic tetraacetylene may be favored in the thermal cyclodimerization of tetraalkyl[5]cumulenes.[6]

Table I. Reaction of Tetraarylhexapentaene **1a–c** with Nickel(0) Complexes

starting material	Ni(0) complex	mol %	solv	temp (°C)	time (min)	yield (%) 2	3
1a	$Ni(PPh_3)_4$[a]	50	THF	25	60	53	0
1a	$Ni(PPh_3)_4$[a]	50	DMF	25	10	41	3
1a	$Ni(PPh_3)_4$[a]	20	DMF	25	30	64	0
1a	$Ni(PPh_3)_4$[a]	50	benzene	25	60	40	10
1a	$Ni(CO)_2(PPh_3)_2$	10	benzene	80	30	61	0
1b	$Ni(CO)_2(PPh_3)_2$	25	benzene	80	30	57	0
1c	$Ni(CO)_2(PPh_3)_2$	50	benzene	80	30	13[b]	0
1c	$Ni(CO)_2(PPh_3)_2$	100	benzene	80	30	34	0

[a] Prepared from $NiBr_2(PPh_3)_2$, PPh_3, and zinc in a 1:2:4 molar ratio. [b] The starting material (23%) was recovered.

Scheme I

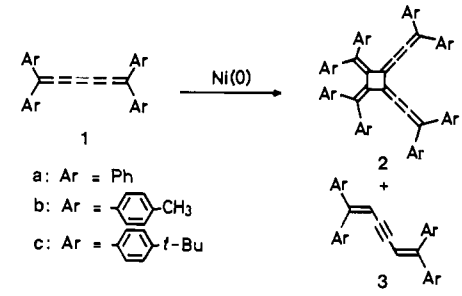

The thermal reaction of tetraarylhexapentaenes has never been reported to give cyclic dimers, presumably owing to thermal instability of these [5]cumulenes. Therefore, we investigated the cyclodimerization of tetraarylhexapentaenes with zero-valent nickel catalysts. As shown in Table I, the reaction of tetraphenylhexapentaene (**1a**) with $Ni(PPh_3)_4$ proceeds smoothly at room temperature to give the cyclic dimer **2a**[7,8] in 40–64% yields. This cyclization gave the same dimer in THF, DMF, and benzene as the solvent, and the formation of the reduction product **3a**[9] was observed as byproduct in the reaction in benzene. As for the nickel catalysts, $Ni(CO)_2(PPh_3)_2$[3] can be also employed for the dimerization of **1a**. Thus, treatment of **1a** with 10 mol % of $Ni(CO)_2(PPh_3)_2$ in refluxing benzene afforded **2a** in 61% yield. Under similar reaction conditions, dimerization of tetrakis(4-methylphenyl)hexapentaene (**1b**)[10] produced **2b**[11] in 57% yield.

(1) For general reviews, see: (a) Jolly, P. W. In *Comprehensive Organometallic Chemistry*; Wilkinson, G., Stone, F. G. A., Abel, E. W., Eds.; Pergamon: Oxford, 1982; Vol. 8, pp 664–668. (b) Jolly, P. W.; Wilke, G. *The Organic Chemistry of Nickel*; Academic: New York, 1975.
(2) (a) Otsuka, S.; Mori, K.; Imaizumi, F. *J. Am. Chem. Soc.* **1965**, *87*, 3017–3019. (b) Otsuka, S.; Mori, K.; Suminoe, T.; Imaizumi, F. *Eur. Polym. J.* **1967**, *3*, 73–83. (c) Hoover, F. W.; Lindsey, R. V., Jr. *J. Org. Chem.* **1969**, *34*, 3051–3052. (d) Otsuka, S.; Nakamura, A.; Tani, K.; Ueda, S. *Tetrahedron Lett.* **1969**, 297–300. (e) De-Pasquale, R. J. *J. Organomet. Chem.* **1971**, *32*, 381–393. (f) Otsuka, S.; Tani, K.; Yamagata, T. *J. Chem. Soc., Dalton Trans.* **1973**, 2491–2497. (g) Pasto, D. J.; Huang, N.-Z. *Organometallics* **1985**, *4*, 1386–1395. (h) Pasto, D. J.; Huang, N.-Z.; Eigenbrot, C. W. *J. Am. Chem. Soc.* **1985**, *107*, 3160–3172.
(3) (a) Iyoda, M.; Tanaka, S.; Nose, M.; Oda, M. *J. Chem. Soc., Chem. Commun.* **1983**, 1058–1059. (b) Iyoda, M.; Tanaka, S.; Otani, H.; Nose, M.; Oda, M. *J. Am. Chem. Soc.* **1988**, *110*, 8494–8500.
(4) (a) Hartzler, H. D. *J. Am. Chem. Soc.* **1966**, *88*, 3155–3156; **1971**, *93*, 4527–4531. (b) Negi, T.; Kaneda, T.; Mizuno, H.; Toyoda, T.; Sakata, Y.; Misumi, S. *Bull. Chem. Soc. Jpn.* **1974**, *47*, 2398–2405.
(5) (a) Scott, L. T.; DeCicco, G. J. *Tetrahedron Lett.* **1976**, 2663–2666. (b) Santiago, C.; Houk, K. N.; DeCicco, G. J.; Scott, L. T. *J. Am. Chem. Soc.* **1978**, *100*, 692–696.
(6) Kaftory, M.; Agmon, I.; Ladika, M.; Stang, P. J. *J. Am. Chem. Soc.* **1987**, *109*, 782–787, and references cited therein.
(7) **2a**: deep blue needles, mp 210 °C dec; MS, *m/z* 760 (M^+); ^1H NMR (500 MHz, $CDCl_3$) δ 7.34–7.29 (m, 10 H), 7.11–7.06 (m, 14 H), 6.98 (t, J = 8.0 Hz, 2 H), 6.88 (t, J = 8.0, 2 H), 6.83 (d, J = 8.0, 4 H), 6.73 (t, J = 8.0, 4 H), 6.68 (t, J = 8.0, 4 H); ^{13}C NMR (125 MHz, $CDCl_3$) δ 147.8, 141.1, 140.5, 139.5, 138.7, 138.4, 136.7, 136.5, 131.0, 130.7, 130.2, 129.5, 129.2, 129.0, 128.3, 127.8, 127.7, 127.6, 127.43, 127.36, 127.2, 123.1; UV-vis (THF) λ_{max} (log ϵ) 230 (4.63), 293 (4.58), 384 sh (4.76), 413 (4.95), 623 nm (4.22); IR (KBr) 2028, 1970 cm^{-1}; Raman (KBr) 2030, 1970 cm^{-1}.
(8) Satisfactory elemental analyses were obtained on all new compounds except for **2c**.
(9) Kuhn, R.; Fischer, H. *Chem. Ber.* **1961**, *94*, 3060–3071.
(10) Kuhn, R.; Platzer, G. *Chem. Ber.* **1940**, *73*, 1410–1417. (b) Ried, W.; Schlegelmilch, W.; Piesch, S. *Chem. Ber.* **1963**, *96*, 1221–1228.
(11) **2b**: dark blue needles, mp 210 °C dec; MS, *m/z* 872 (M^+); ^1H NMR (500 MHz, $CDCl_3$) δ 7.23 (d, J = 8.0, 4 H), 7.06 (d, J = 8.2, 4 H), 7.05 (d, J = 8.2, 4 H), 6.99 (d, J = 8.2, 4 H), 6.88 (d, J = 8.0, 4 H), 6.69 (d, J = 8.0, 4 H), 6.54 (d, J = 8.2, 4 H), 6.52 (d, J = 8.0, 4 H), 2.42 (s, 6 H), 2.17 (s, 6 H), 2.14 (s, 6 H), 2.12 (s, 6 H); UV-vis (THF) λ_{max} (log ϵ) 238 (4.64), 310 (4.62), 385 sh (4.66), 424 (4.97), 694 nm (4.21); Raman (KBr) 2029, 1972 cm^{-1}.

0002-7863/89/1511-3761$01.50/0